Carbohydrate Polymers 82 (2010) 1061–1067

Contents lists available at ScienceDirect

Carbohydrate Polymers

journal homepage: www.elsevier.com/locate/carbpol

Effect of polyglycerol and the crosslinking on the physical properties of a blend alginate-hydroxyethylcellulose

R. Russo*, M. Abbate, M. Malinconico, G. Santagata

Institute of Chemistry and Technology of Polymers – CNR, Via Campi Flegrei, 34 – 80078 Pozzuoli (NA), Italy

ARTICLE INFO

Article history:
Received 29 March 2010
Received in revised form 15 June 2010
Accepted 16 June 2010
Available online 26 June 2010

Keywords:
Alginate
Hydroxyethylcellulose
Polyglycerol
Physical properties
SEM

ABSTRACT

Films of pure sodium alginate and films containing sodium alginate with hydroxyethylcellulose and/or polyglycerol were prepared in order to study their effect on the physical properties. In addition, the films, with different composition, were ionically crosslinked with calcium ions by soaking the films in a solution of calcium chloride. The films containing hydroxyethylcellulose are homogeneous with good mechanical properties. The addition of hydroxyethylcellulose and polyglycerol modifies in a noticeable way some thermal and mechanical parameters, but also the amount of water absorbed in terms of bound water and free water.

1. Introduction

In the past two decades the use of natural polymers, coming from renewable sources, increased substantially. Because of the high post-consumer plastic waste, produced every year, and the reduced availability of landfills, biodegradability is one of the most attractive properties of this class of materials. The replacement of synthetic polymers in many applications with natural polymers reduces the problem of disposability of traditional plastics and, at the same time, reduces the dependence on petroleum (Scott, 2000; Bastioli, 1997; Nayak, 1999; Wang, Yang, & Wang, 2003; Briassoulis, 2006a, 2006b).

Since in many cases the properties of natural polymers do not fit the needs for specific applications, the blending with other natural polymers and/or synthetic biodegradable polymers is a route largely used to gain the desired properties (Immirzi, Malinconico, Romano, Russo, & Santagata, 2003; Russo, Giuliani, Immirzi, Malinconico, & Romano, 2004; Russo, Malinconico, Petti, & Romano, 2005; Xiao, Lu, Liu, & Zhang, 2000).

The aim of this study is to analyze how some physical properties of films of sodium alginate (A) are influenced when blended with hydroxyethylcellulose (HEC) and/or polyglycerol (PG). Physical properties of ionically crosslinked films are also analyzed.

Alginates are well known natural ionic polysaccharides used mainly as food additives, thickener, gelling agent, and in the controlled delivery of drugs (Gombotz & Wee, 1998; Gomez-Diaz & Navata, 2004; Holte, Onsoyen, Myrvold, & Karlsen, 2003). Recently, blends and composites containing alginates have been used to prepare hydrophilic membranes for pervaporation, which is a membrane based process used for the separation of liquid mixtures including azeotropic mixtures (Aminabhavi et al., 2009; Kalyani, Smitha, Sridhar, & Krishnaiah, 2006; Krishna Rao, Vijaya Kumar Naidu, Subha, Sairam, & Mallikarjuna, 2006; Krishna Rao, Lokesh, Srinivasa Rao, & Chowdoji Rao, 2008; Kumar Naidu, Sriram, Raju, & Aminabhavi, 2005; Veerapur et al., 2007; Vijaya Kumar Naidu, Krishna Rao, & Tejraj, 2005).

Alginates are linear water-soluble polysaccharides comprising (1 → 4)-linked units of α-D-mannuronate (M) and β-L-guluronate (G) at different ratio and different distribution in the chains (Draget, Skiak-Braek, & Smidsrod, 1997; Grasdalen, Larsen, & Smidsrod, 1981). They are present in brown algae and can also be found in metabolic products of some bacteria (Wingender, Neu, & Flemming, 1999). The chemical composition and sequence of the M and G residues depend on the biological source and the state of maturation of the plant (Moe, Draget, Skiak-Braek, & Smidsrod, 1995). The alginates, as well as all the polysaccharides, are polydispersed in terms of molecular mass (Smidsrod, Glover, and Whittington, 1973).

For several applications in which films containing alginate are used, the crosslinking is necessary (Smidsrod, 1974). Alginate chains can be crosslinked in the presence of divalent ions, where the divalent ions cooperatively interact with blocks of guluronic units to form ionic bridges between different chains (Draget, Skiak-Braek, & Stokke, 2006; Gomez-Diaz & Navata, 2004). The ability of

* Corresponding author.
E-mail address: russo@ictp.cnr.it (R. Russo).

0144-8617/$ – see front matter © 2010 Elsevier Ltd. All rights reserved.
doi:10.1016/j.carbpol.2010.06.037

Table 1
Sample composition.

Sample	A (g)	HEC (g)	PG (g)
A	3.00	–	–
A-PG	3.00	–	1.00
A75	2.25	0.75	–
A75-PG	2.25	0.75	1.00
HEC	–	3.00	

forming this kind of interaction depends on the length of the G-blocks. The most popular model to account for the chain-to-chain association is the "egg box model" (Grant, Morris, Rees, Smith, & Thom, 1973; Morris, Rees, Thom, & Boyd, 1978). In this model the G-blocks form a three-dimensional arrangement in which Ca ions are embodied in cavities like eggs in a cardboard egg-box. Instead, according to some authors, it seems that the Ca ion can be localized in different special arrangements, still promoting the lateral association (Chandrasekaran, Puijaner, Joyce, & Arnott, 1988; Mackie, Perez, Rizzo, & Vignon, 1983; Stokke et al., 2000).

The alginate can be considered a block copolymer containing three types of blocks (GG, MM, and MG). The stiffness of the three blocks decreases in the order GG > MM > MG (Chandrasekaran et al., 1988). The physical and chemical properties of alginates strictly depend on their composition and the sequence of guluronic and mannuronic residues in the polymeric chain (Draget et al., 2006). In a recent paper we have analyzed the properties of three films of alginates, with different ratio G-blocks/M-blocks, crosslinked with calcium ions (Russo, Malinconico, & Santagata, 2007).

Hydroxyethylcellulose is a non-ionic water-soluble cellulose ether, which is compatible with a wide range of water-soluble polymers. It forms homogeneous blends with alginate (Vijaya Kumar Naidu et al., 2005). Polyglycerol consists of glycerol molecules bonded by an ether linkage.

In this study we analyzed films of pure alginate and a blend with hydroxyethylcellulose, with and without polyglycerol, in order to understand their effect on the physical properties of alginate. The effect of crosslinking with calcium ions is also analyzed.

2. Materials and methods

2.1. Materials and film preparation

Sodium alginate (A), with $37 \pm 1\%$ of guluronic fraction, $M_n = 2.3 \times 10^5$ Da and $M_w = 1.2 \times 10^6$ Da, was purchased from Lianyungang Zhongda Seaweed Industrial Co. Ltd. (China).

Hydroxyethylcellulose (HEC), with $M_w = 2.5 \times 10^5$ Da, with D.S. = 1.0 mol per mol of cellulose and M.S. = 2.0 mol per mol of cellulose was purchased from Aldrich.

Polyglycerol (PG), a mixture containing a minimum of 85% diglycerol, triglycerol and tetraglycerol with only trace amounts of glycerol, was purchased from Solvay.

All films were prepared by casting from aqueous solutions. The films were obtained by dissolving the ingredients in 200 mL of distilled water, under stirring, at the temperature of 70–75 °C. All solutions were filtered and kept for a few minutes under vacuum. After this treatment the solutions were poured, avoiding bubble formation, into a glass mold kept in plane to ensure the homogeneous thickness of the films. The compositions of the films are reported in Table 1. The code A corresponds to a film of pure alginate, the code A-PG refers to the film of A containing PG, the code A75 refers to film containing 75% of A and 25% of HEC, the code A75-PG refers to the film at 75% of A containing PG. In samples A-PG and A75-PG, the amount of polyglycerol is 25%. The code HEC refers to the film of pure HEC. The films thicknesses, were in the range of 70–80 μm. All films were allowed to form during exposure to the atmosphere for three days. Prior to testing, the films were equilibrated at 45% relative humidity by storing them in a desiccator over a saturated solution of calcium nitrate at room temperature. The crosslinked samples were prepared by soaking for 30 min the films in a 2% (w/v) aqueous solution of calcium chloride. The crosslinking with calcium ions involves only the alginate chains. We add the symbol of calcium Ca, to the codes, to distinguish the crosslinked samples.

2.2. Determination of the thickness

The thickness was determined with Juwel Electronic Digital Micrometer with accuracy of 0.001 mm.

2.3. Scanning electron microscopy (SEM)

Scanning electron microscopy of sample surfaces was performed by means of a FEI Quanta 200 FEG SEM (FEI, Eindhoven, The Netherlands).

Air dried samples were fixed onto aluminum stubs through carbon adhesive disks and observed with a low-vacuum secondary electron detector using the accelerating voltage of 5.0 kV. The samples were observed at room temperature and at an internal pressure of 0.50 torr.

2.4. Differential scanning calorimetry (DSC)

DSC measurements were carried out on samples of 7–8 mg over a temperature range of 0–400 °C using a Mettler TA 3000 DSC purged with nitrogen and chilled with liquid nitrogen, with a heating rate of 10 °C/min. All the samples, before the run, were kept in the DSC for 2 h at 110 °C to allow the elimination of some water that would mask the T_g of alginates. The data were confirmed on a second set of samples.

2.5. Thermogravimetric analysis

Thermogravimetric analyses were carried out with a Mettler Thermogravimetric Analyzer Mod. TG 50. The measurements were performed on samples of about 8–10 mg, placed in ceramic crucibles, from 30 to 400 °C at a heating rate of 10 °C/min, under nitrogen atmosphere with a nominal gas flow rate of 25 mL/min. For each composition the thermogravimetric tests were performed in duplicate.

2.6. Mechanical analysis

Young's moduli and stress–strain curves were determined at room temperature with an Instron 4301 tensile testing machine. The measurements were performed on samples 70–80 μm thick, 6–7 mm wide, and 15–20 mm long. The temperature of the experiment was 20 °C, and the relative humidity was in the range 45–50%. The extension rate was 2 mm/min for the determination of moduli and 10 mm/min for the stress–strain curves.

For each composition five specimens were tested and Young's modulus E, stress at break σ_b, and elongation at break ε_b values were thus obtained. The reported data are the means of five samples. The values of the Young's modulus are within ±10%, while the stress values are within ±15%, and the elongation at break fluctuates in the range of ±20%.

2.7. Dynamic-mechanical analysis (DMA)

DMA tests were carried out in duplicate on a Perkin Elmer Pyris Diamond DMA in tensile mode at a frequency of 1 Hz in the range

Table 2
Change of thickness as effect of crosslinking.

Sample	Thickness before crosslinking (μm)	Thickness after crosslinking (μm)	Thickness increase (%)
A	74	107	45
A-PG	80	110	38
A75	75	118	57
A75-PG	81	125	54

of −100 to 250 °C, under nitrogen atmosphere, at a heating rate of 3 °C/min.

2.8. Infrared spectroscopy

Fourier Transform Infrared Spectroscopy (FTIR) measurements were performed by a Perkin-Elmer System 2000 spectrometer, equipped with a deuterated triglycine sulphate (DTGS) detector and a Ge/KBr beam splitter. 32 spectra were signal averaged in the conventional manner to reduce the noise.

Attenuated Total Reflectance (FTIR-ATR) spectra were collected in the medium infrared region (MIR: 4000–700 cm^{-1}) by using a horizontal ATR cell (Benchmark from Graseby Specac) having a ZnSe crystal. This unit was equipped with a temperature controlling system having an accuracy of ±0.5 °C.

3. Results and discussion

3.1. Swelling Phenomena

The thickness of all the samples, except HEC, was measured before and after the immersion for 30 min in a 2% (w/v) aqueous solution of calcium chloride. The data are reported in Table 2. The samples swelled and at the same time crosslinked. The thickness of crosslinked samples was measured after drying and conditioning them at room temperature at 45% relative humidity. The thicknesses of the original samples increased by 45–60%. As already reported in a previous study (Russo et al., 2007), the thickness increased because the crosslinking points, introduced in a swollen state, stabilize the conformations of this state.

3.2. Scanning electron microscopy (SEM)

In Fig. 1 the surface of the film A75 (a) and A75-Ca (b) are reported. As already found by other authors (Vijaya Kumar Naidu et al., 2005) A and HEC form compatible blends. This is confirmed by the smoothed surface of the film (Fig. 1a). The surface of the film of sample A75-Ca, instead, is rough (Fig. 1b). This is due to the fact that, when the sample is soaked in a solution of calcium chloride, it swells and this state is stabilized by the crosslinking points.

3.3. Differential scanning calorimetry (DSC)

In the DSC heating curves we have two regions of interest: the first in the temperature range 100–150 °C, in which the elimination of most of the water and the glass transition occur, and the second region, above 180 °C, concerning the decomposition.

We are confident that, under nitrogen flux, the decomposition of the samples, occurs at temperatures above 180 °C. In order to prove this, three consecutive runs on the samples of each composition from room temperature to 180 °C were performed. In the first run a broad endotherm peak, related to the elimination of water, is recorded. Once the majority of water is eliminated, the second and the third run are identical, proving in this way, that below 180 °C, in inert atmosphere, the degradation process does not take place.

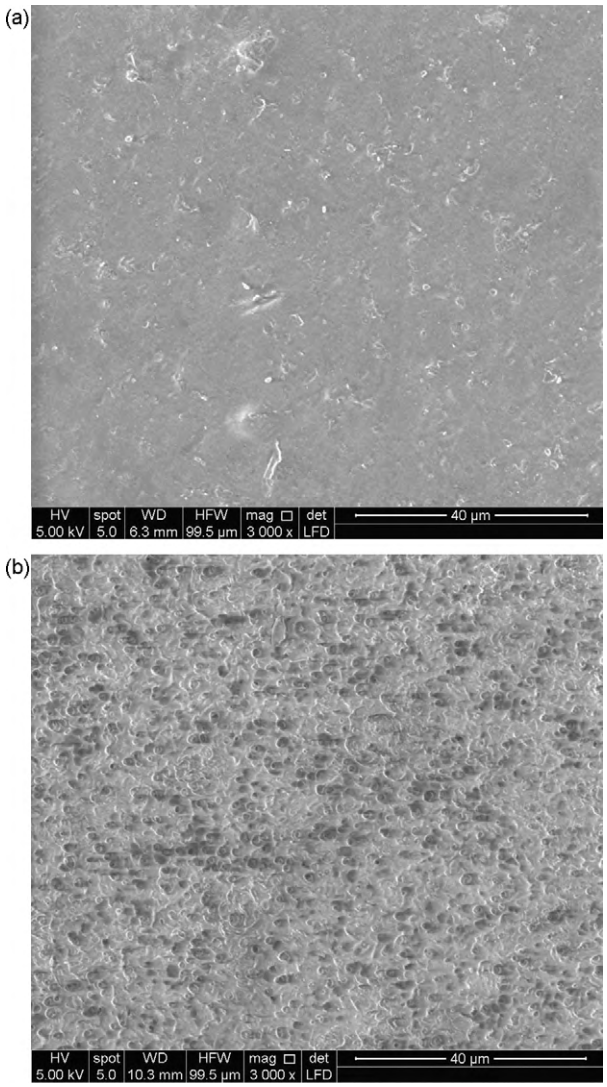

Fig. 1. SEM images of (a) A75 and (b) A75-Ca.

The glass transition temperature of our system, in samples containing water, is not detectable. In fact, the endotherm related to the elimination of water, covers any signal related to the glass transition. For this reason, before each run, the samples were kept in the DSC at a temperature of 110 °C for 2 h under nitrogen purge. After the elimination of most of the water, the glass transition temperature is easily detectable. The glass transition temperatures T_g for the uncrosslinked samples are reported in Table 3.

From the data we notice two effects. The first is the reduction of T_g when HEC is added to the alginate to form the blend A75. The T_g of A75 is lower than the T_g of either A or HEC. This is not surprising if we consider that when the two polymers are mixed there is an increase of the free volume with respect to the pure polymers. The second effect deals with the addition of PG. Because of the low molecular mass of PG one would have expected a plasticizing effect with a consequent reduction of the T_g. Although the low molecular mass of PG, the high density of hydroxyl groups promotes the interaction, via hydrogen bonding, among the chains. The presence of PG therefore exerts a hindering effect that reduces the molecular mobility with a consequent increase of T_g. Also for the sample A75 the addition of PG causes an increase of T_g.

The T_g of crosslinked samples is not reported in the table since for these samples the change of heat capacity occurs over a larger interval of temperature and therefore not clearly detectable.

Table 3
Mass loss at different temperatures and glass transition temperature.

Sample	Mass loss at 80 °C (%)	Mass loss at 100 °C (%)	Mass loss at 140 °C (%)	Mass loss at 180 °C (%)	T_g (°C)
A	11.1	13.0	15.6	17.6	137
A-PG	7.7	10.6	14.8	17.1	155
A75	9.6	12.3	14.8	16.6	124
A75-PG	5.8	9.5	13.2	14.8	137
HEC	7.5	7.6	8.0	8.0	131

3.4. Thermogravimetric analysis

The thermogravimetric data are reported in Table 3, Figs. 2 and 3. A and HEC are different both in terms of sorbed water and in terms of thermal decomposition. In the thermogravimetric curves we can distinguish three regions. The first from room temperature to 100 °C, the second between 100 °C and 200 °C, and the third at temperatures above 200 °C. In the first and the second region the mass loss is associated with the elimination of water, while in the third region the mass loss is associated to the degradation.

It has been reported, by different authors, that there are three kinds of absorbed water in hydrophilic polymers: free, freezing bound and non-freezing water or bound water (Hatakeyama, Nakamura, & Hatakeyama, 1995, Kim, Yoon, & Kim, 2004; Nakamura, Hatakeyama, & Hatakeyama, 1983). Free water does not interact, via hydrogen bonding, with the polymeric chain, it behaves as pure water. The freezing bound water interacts only weakly with the polymeric chain, while the non-freezing water is represented by molecules of water bound to the polymeric chains through hydrogen bonds. This kind of water does not show any first-order phase transition.

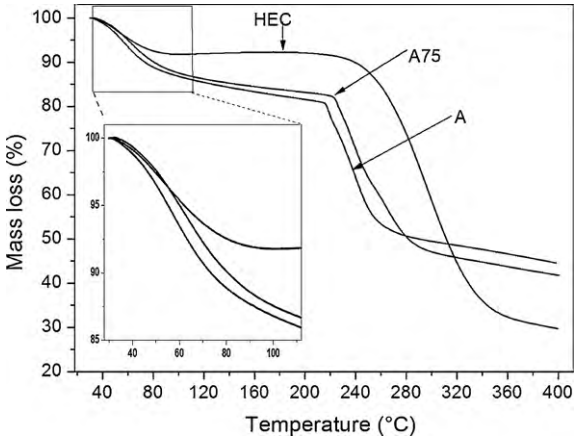

Fig. 2. Thermogravimetric curves of samples A, HEC, and A75.

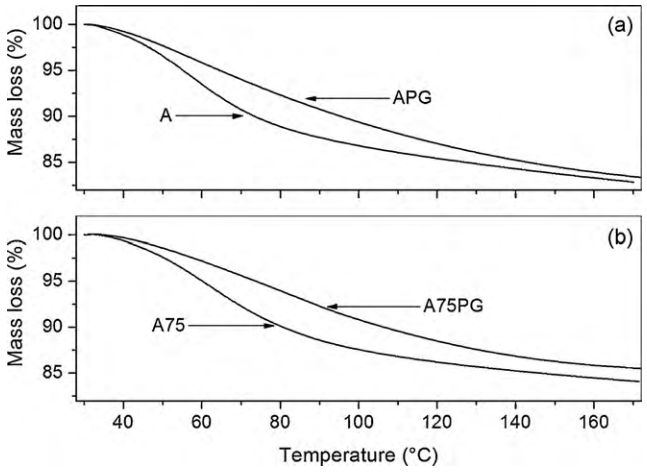

Fig. 3. Thermogravimetric curves of (a) samples A and APG and (b) sample A75 and A75-PG.

The mass loss in the first region can be ascribed to the elimination of free water. These molecules of water are the first molecules leaving the sample. Above 100 °C the samples still contain water. In fact, on increasing the temperature, the mass of the samples continues to decrease, although the decomposition processes have not been involved yet. The second and the third type of water are released in this region.

From Fig. 2 and Table 3 we notice that at 180 °C, a temperature at which the degradation process has not begun yet, sample A releases about 18% of water, while HEC only 8%. Moreover, while HEC releases all the water at temperatures below 80 °C, A looses about 11% of water at $T < 80$ °C and the residual 7% in the interval 80–180 °C. It means that, while in HEC the absorbed water is basically free water, in A we have either free or bound water. This noticeable difference is related to the different chemical nature of the two polymers. While in HEC we have only the hydroxyl groups able to interact with molecules of water, in A, in addition to the hydroxyl groups, we also have carboxylic groups. The larger amount of water absorbed by A is therefore compatible with the presence of either hydroxyl groups or carboxylic group. The presence of bound water in A is justified by the presence of $-COO^-$ groups. The curve of the blend A75 interpolates between the pure polymers A and HEC.

The addition of PG to the pure alginate or to the blend affects the interaction with the water. In particular we notice from Fig. 3 and the data in Table 3 that the addition of PG does not appreciably affect the amount of absorbed water, but the amount of bound water increases in samples containing PG. The high density of OH groups in PG could be responsible of the increased amount of bound water in A-PG and in A75-PG. In A-PG, the water released at $T < 80$ °C is about 3% less than in A, while in A75-PG the water released at $T < 80$ °C is about 4% less than in A75.

As for the degradation, we notice that A is more susceptible than HEC. The crosslinked samples exhibit an increased susceptibility towards the decomposition. The degradation is anticipated by 10–15 °C. The lower temperature at which the degradation starts can be related to the increased volume of samples containing calcium. The less packed chains are more vulnerable to the degradation.

3.5. Mechanical analysis

The stress–strain curves are reported in Fig. 4 and the data are summarized in Table 4. From the data we notice that the addition of HEC to A, as expected, causes a decrease of the Young's modulus and the stress level during the deformation. The addition of PG causes a further decrease of the Young's modulus and the stress level in the stress–strain curves. In the DSC measurements we noticed that the addition of PG caused an increase of the T_g. The reduction of the mechanical parameters and a correspondent increase of T_g, as effect of the addition of PG, seems a contradiction, but we offer a possible explanation. At molecular level there is a difference between

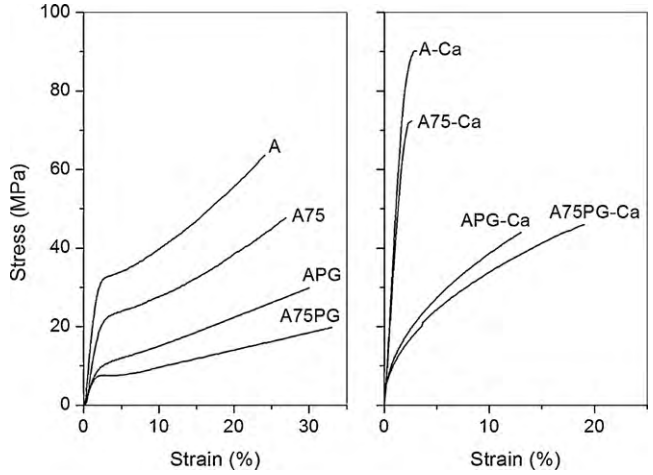

Fig. 4. Stress–strain curves.

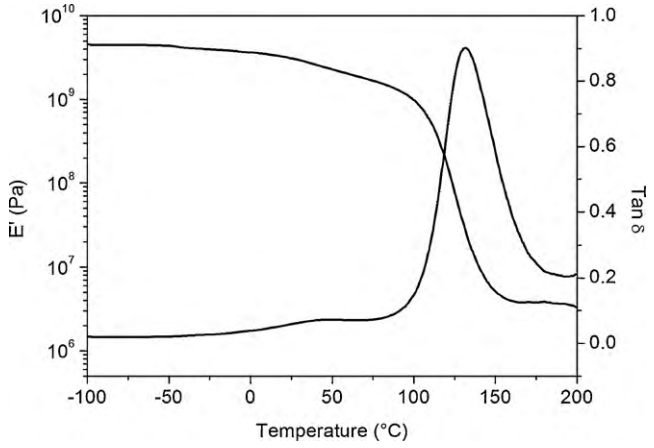

Fig. 5. Storage modulus and tan δ of samples HEC.

the T_g and the Young's modulus. While at T_g the long range motion of segments of chains is possible, the determination of the elastic modulus involves deformations at short range. The two phenomena are not easy to correlate since we are in different temperature ranges. In our systems the long range mobility occurs at temperatures above 120 °C, while we determined the Young's modulus at room temperature. The presence of PG, at room temperature, represents just a defect for samples in the glassy state, which reduces the stiffness of our material. In other words the antiplasticizing effect of PG is evident only when the system is above the T_g. Further work is in progress to better investigate this point.

As expected, the crosslinking causes an increase of the Young's modulus and a decrease of the elongation at break.

3.6. Dynamic-mechanical analysis

The storage modulus (E') and the loss factor tan δ for HEC is reported in Fig. 5. E' and tan δ for samples A, A75 and APG are reported in Fig. 6. All the runs were performed on samples kept for 2 h at 110 °C in order to remove most of the water and, therefore, to better visualize the transitions. HEC and A are quite different in terms of E' and tan δ. The modulus of A remains constant in a wide range of temperatures, while in HEC the decline of the modulus starts at about 20 °C followed by the drop at T_g. As for the tan δ we notice that all the samples have a transition above 100 °C due to the glass transition (α transition). HEC has a net peak centered at 131 °C, while A and A75 show only a shoulder in this range of temperatures. The reason for this difference is due to the different decomposition temperatures of HEC and A. The peak of tan δ is pretty neat in HEC since it is not biased by the onset of the decomposition. In fact, as seen in Fig. 2, the onset of the decomposition for HEC occurs at about 240 °C, while in A the decomposition starts at about 210 °C. The broad transition at low temperatures (β transition) in sample A, already described in a recent paper (Russo et al., 2007), and also suggested by other authors (Krumova, Lopez, Benavente, Mijangos, & Perena, 2000), is related to the motion of hydroxyl groups connected to water molecules.

The presence of PG does not modify the profile of tan δ in a significant way. As already found with the mechanical testing, the addition of HEC and PG causes a decrease of the storage modulus (Fig. 6a).

Table 4
Mechanical data Young's modulus (E), stress at break (σ_b), elongation at break (ε_b).

Sample	E ±10% (MPa)	σ_b ±15% (MPa)	ε_b ±20% (%)
A	2030	64	24
A75	1190	48	27
HEC	30	12	60
A-PG	650	30	30
A75-PG	580	20	33
A-Ca	4350	90	3
A-PG-Ca	4550	73	3
A75-Ca	2800	38	13
A75-PG-Ca	3120	47	19

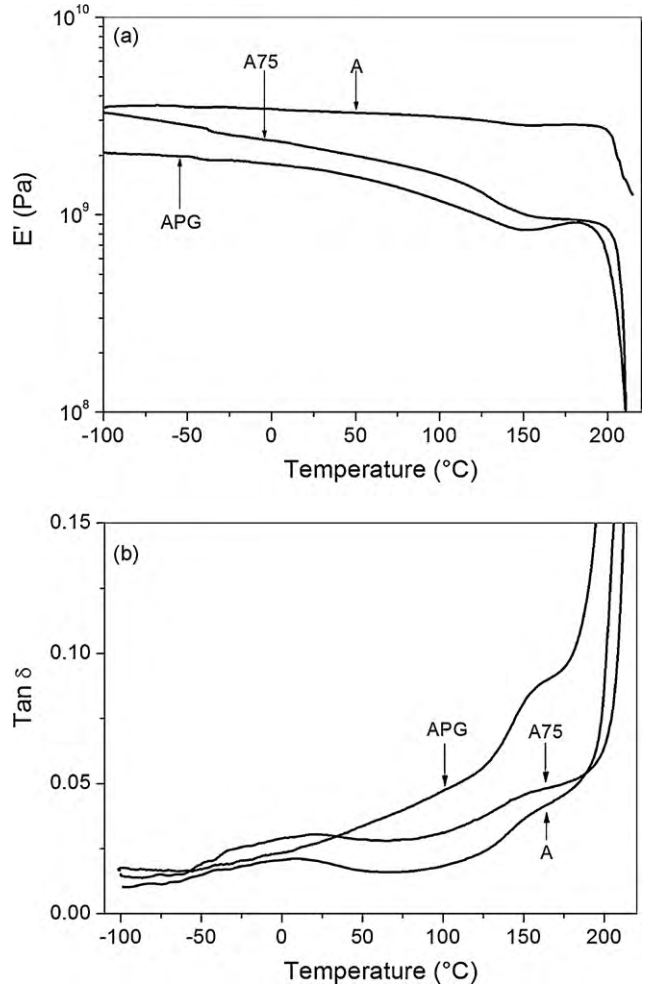

Fig. 6. Storage modulus (a) and tan δ (b) for samples A, A75, and APG.

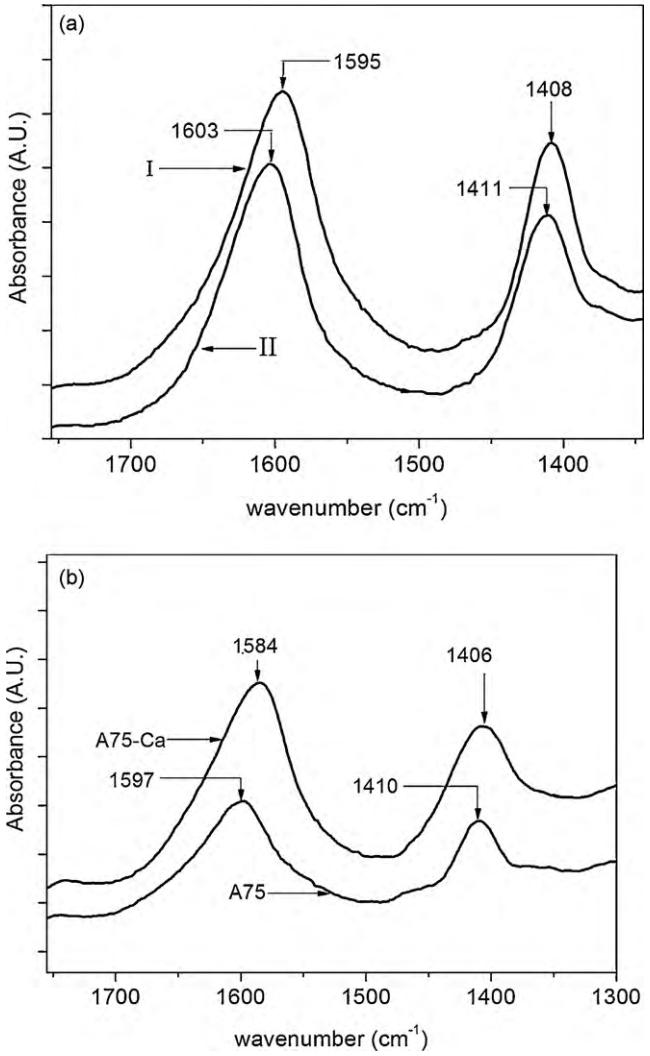

Fig. 7. (a) Infrared spectrum of A (I), and A after the thermal treatment (II), (b) infrared spectrum of A75 and A75-Ca.

3.7. Infrared spectroscopy

Spectra of A and A75 are reported in Fig. 7. The spectrum of A shows the characteristic peaks in the range 1595–1610 cm^{-1} and in the range 1405–1415 cm^{-1} due to the COO^- asymmetric and symmetric stretchings. In the fingerprint region there are several absorptions used to estimate the ratio mannuronic/guluronic (Sartori, Finch, Ralph, & Gilding, 1997; Sakugawa, Ikeda, Takemura, & Ono, 2004). In the HEC spectrum we do not notice specific features with respect to the spectrum of A. Both spectra show characteristic peaks in the range 3200–3550 cm^{-1} corresponding to O–H stretching vibrations.

The spectra were detected at room temperature and after the samples were kept for 2 h at 110 °C in order to remove most of the water and to see how the molecules of water interact with the alginate chains. The spectra, after the thermal treatment at 110° for 2 h, were recorded again at room temperature. The thermal treatment caused shifts of the peaks assigned to the stretching of the group COO^- indicating the interaction between the molecules of water and the carboxylic groups. In Fig. 7a we see the shift of the bands assigned to the stretching of the group COO^- towards larger wavenumbers for sample A after the thermal treatment. A similar effect is also observed when PG is added. Because of the high density of the hydroxyl groups in PG the shifts of the stretching of the carboxylic groups is a confirmation of the strong interaction between the molecules of PG and the alginate chains.

The crosslinking with calcium ions causes a change of the spectra. In Fig. 7b we report the spectra of sample A75 and A75-Ca in the region 1750–1300 cm^{-1}. In particular we notice that the peaks assigned to stretching of the group COO^- move to lower wavenumbers, as an effect of the crosslinking, indicating a strong interaction between the carboxylic group and the calcium ions.

4. Conclusions

In this work the physical behavior of films based on sodium alginate have been studied. In particular we have studied how the physical properties of films of pure alginate are modified by the presence of hydroxyethylcellulose, and polyglycerol. Alginate and hydroxyethylcellulose have different physical properties and a different ability to absorb molecules of water either in terms of quantity or in terms of interaction with the polymeric chains. The introduction of polyglycerol does not modify the amount of the total absorbed water, but the fraction of bound water increases in the presence of PG. The presence of PG increases the temperature of the glass transition, but lowers the Young's modulus and the stress level during the deformation. The crosslinking causes a noticeable increase of the free volume. The interaction with the polyglycerol and the effect caused by the crosslinking with calcium ions have also been checked with the shift of some infrared bands.

Acknowledgment

The authors wish to thank Dr. Gennaro Gentile for his assistance in performing the SEM observations.

References

Aminabhavi, T. M., Patil, M. B., Bhat, S. D., Halgeri, A. B., Vijayalakshmi, R. P., & Kumar, P. (2009). Activated charcoal-loaded composite membranes of sodium alginate in pervaporation separation of water-organic azeotropes. *Journal of Applied Polymer Science*, *113*, 966–975.

Bastioli, C. (1997). Biodegradable materials—Present situation and future perspectives. *Macromolecular Symposia*, *135*, 193–204.

Briassoulis, D. (2006a). Mechanical behavior of biodegradable agricultural films under real field conditions. *Polymer Degradation and Stability*, *91*, 1256–1272.

Briassoulis, D. (2006b). Mechanical performance and design criteria of biodegradable low-tunnel films. *Journal of Polymers and the Environment*, *14*, 289–307.

Chandrasekaran, R., Puijaner, L. C., Joyce, K. L., & Arnott, S. (1988). Cation interactions in gellan: An X-ray study of the potassium salt. *Carbohydrate Research*, *181*, 23–40.

Draget, K. I., Skiak-Braek, G., & Smidsrod, O. (1997). Alginate based new material. *International Journal of Biological Macromolecules*, *21*, 47–55.

Draget, K. I., Skiak-Braek, G., & Stokke, B. T. (2006). Similarities and differences between alginic acid gels and ionically crosslinked alginate gels. *Food Hydrocolloid*, *20*, 170–175.

Gombotz, W. R., & Wee, S. F. (1998). Protein release from alginate matrices. *Advanced Drug Delivery Review*, *31*, 267–285.

Gomez-Diaz, D., & Navata, J. M. (2004). Rheology of food stabilizers blends. *Journal of Food Engineering*, *64*, 143–149.

Grant, G. T., Morris, E. R., Rees, D. A., Smith, P. J. C., & Thom, D. (1973). Characterization of alginate composition and block-structure by circular dicroism. *FEBS Letters*, *32*, 195–198.

Grasdalen, H., Larsen, B., & Smidsrod, O. (1981). ^{13}C-NMR Studies of monomeric composition and sequence in alginate. *Carbohydrate Research*, *89*, 179–191.

Hatakeyama, T., Nakamura, K., & Hatakeyama, H. (1995). Non-freezing water content of mono- and divalent cation salts of polyelectrolyte–water systems studied by DSC. *Thermochimica Acta*, *253*, 137–148.

Holte, O., Onsoyen, E., Myrvold, R., & Karlsen, J. (2003). Sustained release of water-soluble drug from directly compressed alginate tablets. *European Journal of Pharmaceutical science*, *20*, 403–407.

Immirzi, B., Malinconico, M., Romano, G., Russo, R., & Santagata, G. (2003). Biodegradable films of natural polysaccharides blends. *Journal of Material Science Letters*, *22*, 1389–1392.

Kalyani, S., Smitha, B., Sridhar, S., & Krishnaiah, A. (2006). Blend membranes of sodium alginate and hydroxyethylcellulose for pervaporation-based enrichment of *t*-butyl alcohol. *Carbohydrate Polymers*, *64*, 425–432.

Kim, S. J., Yoon, S. G., & Kim, S. I. (2004). Synthesis and characteristics of interpenetrating polymer network hydrogels composed of alginate and poly(diallydimethylammonium chloride). *Journal of Applied Polymer Science*, *91*, 3705–3709.

Krishna Rao, K. S. V., Lokesh, B. G., Srinivasa Rao, P., & Chowdoji Rao, K. (2008). Synthesis and characterization of biopolymeric blend membranes based on sodium alginate for the pervaporation dehydration of isopropanol/water mixtures. *Separation Science and Technology*, *43*(5), 1065–1082.

Krishna Rao, K. S. V., Vijaya Kumar Naidu, B., Subha, M. C. S., Sairam, M., Mallikarjuna, N. N., et al. (2006). Novel carbohydrate polymeric blend membranes in pervaporation dehydration of acetic acid. *Carboydrate Polymers*, *66*, 345–351.

Krumova, M., Lopez, D., Benavente, R., Mijangos, C., & Perena, J. (2000). Effect of crosslinking on the mechanical and thermal properties of poly(vinyl alcohol). *Polymer*, *41*, 9265–9272.

Kumar Naidu, B. V., Sairam, M., Raju, K. V. S. N., & Aminabhavi, T. (2005). Thermal, viscoelastic, solution and membrane properties of sodium alginate/hydroxyethylcellulose blends. *Carboydrate Polymers*, *61*, 52–60.

Mackie, W., Perez, S., Rizzo, R., & Vignon, M. (1983). Aspects of the conformation of polyguluronate in the solid state and in solution. *International Journal of Biological Macromolecules*, *5*, 329–341.

Moe, S. T., Draget, K. I., Skiak-Braek, G., & Smidsrod, O. (1995). Alginates. In A. M. Stephen (Ed.), *Food polysaccharides and their applications*. New York: Marcel Dekker.

Morris, E. R., Rees, D. A., Thom, D., & Boyd, J. (1978). Chiroptical and stoichiometric evidence of a specific, primary dimerisation process in alginate gelation. *Carbohydrate Research*, *66*, 145–154.

Nakamura, K., Hatakeyama, T., & Hatakeyama, H. (1983). Relationship between hydrogen bonding and bound water in polyhydroxystyrene derivatives. *Polymer*, *24*, 871–876.

Nayak, P. L. (1999). Biodegradable polymers: opportunities and challenges. *Journal of Macromolecular Science—Review Macromolecular Chemistry and Physics*, *C39*, 481–505.

Russo, R., Giuliani, A., Immirzi, B., Malinconico, M., & Romano, G. (2004). Alginate/polyvinylalcohol blends for agricultural applications: structure–properties correlation, mechanical properties and greenhouse effect evaluation. *Macromolacular Symposia*, *218*, 241–250.

Russo, R., Malinconico, M., Petti, L., & Romano, G. (2005). Physical behavior of biodegradable alginate-poly(vinyl alcohol) blend films. *Journal of Polymer Science, Part B: Polymer Physics*, *43*, 1205–1213.

Russo, R., Malinconico, M., & Santagata, G. (2007). Effect of cross-linking with calcium ions on the physical properties of alginate films. *Biomacromolecules*, *8*, 3193–3197.

Sakugawa, K., Ikeda, A., Takemura, A., & Ono, H. (2004). Simplified method for estimation of composition of alginates by FTIR. *Journal of Applied Polymer Science*, *93*, 1372–1377.

Sartori, C., Finch, D. S., Ralph, B., & Gilding, B. (1997). Determination of the cation content of alginate thin films by FTIR spectroscopy. *Polymer*, *38*, 43–51.

Scott, G. (2000). 'Green' polymers. *Polymer Degradation and Stability*, *68*, 1–7.

Smidsrod, O. (1974). Molecular basis for some physical properties of alginates in the gel state. *Faraday discussions of the Chemical Society*, *57*, 263–274.

Smidsrod, O., Glover, R. M., & Whittington, S. T. (1973). The relative extension of alginates having different chemical composition. *Carbohydrate Research*, *27*, 107–118.

Stokke, B. T., Draget, K. I., Smidsrod, O., Yuguchi, Y., Urakawa, H., & Kajiwara, K. (2000). Small-angle X-ray scattering and rheological characterization of alginate gels. 1. Ca-alginate gels. *Macromolecules*, *33*, 1853–1863.

Veerapur, R. S., Gudasi, K. B., Sairam, M., Shenoy, R. V., Netaji, M., Raju, K. V. S. N., et al. (2007). Novel sodium alginate composite membranes prepared by incorporating cobalt(III) complex particles used in pervaporation separation of water–acetic acid mixtures at different temperatures. *Journal of Material Science*, *42*, 4406–4417.

Vijaya Kumar Naidu, B., Krishna Rao, K. S. V., Aminabhavi, & Tejraj, M. (2005). Pervaporation separation of water + 1,4-dioxane and water + tetrahydrofuran mixtures using sodium alginate and its blend membranes with hydroxyethylcellulose. A comparative study. *Journal of Membrane Science*, *260*, 131–141.

Wang, X. L., Yang, K. K., & Wang, Y. Z. (2003). Properties of starch blends with biodegradable polymers. *Journal of Macromolecular Science Part C*, *43*, 385–409.

Wingender, J., Neu, T. R., & Flemming, H. C. (1999). *Microbial extracellular polymeric substances*. Berlin/Heidelberg/New York: Springer.

Xiao, C., Lu, Y., Liu, H., & Zhang, L. (2000). Preparation and physical properties of blend films from sodium alginate and polyacrylamide solutions. *Journal of Macromolecular Science—Pure and Applied Chemistry*, *A37*, 1663–1675.